

Theoretical Inhibition Efficiency Study of Schiff Base (*E*)-2-(2-hydroxybenzylideneamino)phenylarsonic Acid and its Isomers

María Eugenia Castro*, M. Judith Percino, Margarita Cerón, Guillermo Soriano, Víctor M. Chapela

Centro de Química, Instituto de Ciencias, Universidad Autónoma de Puebla, Complejo de Ciencias, ICUAP, Edif. 103H, 22 Sur y San Claudio, Ciudad Universitaria. Puebla, Pue.-72570, México.

*E-mail: mareug.castro@correo.buap.mx

Received: 20 August 2014 / Accepted: 25 September 2014 / Published: 28 October 2014

The ability of a series of isomers of the Schiff base (*E*)-2-(2-hydroxybenzylideneamino) phenylarsonic acid to inhibit corrosion is evaluated on the basis of their electronic properties, using their energy levels of the frontier molecular orbitals, dipole moments, and atomic and group charges. The different isomers are obtained by attaching the hydroxy substituent at different positions of the phenyl ring. The molecular electronic properties for each isomer are theoretically calculated by DFT methods in M06L/cc-pVTZ level and using as the basis set for the As atom the effective core potential of Hay and Wadt, LanL2DZ. The relationship between the inhibition efficiency and the molecular structure and electronic properties is evaluated using linear regression analysis. This study provides insights into the effect of the position of the –OH substituents and –AsO₃H₂ on the structure of the Schiff base.

Keywords: Schiff base; corrosion inhibition; DFT theoretical calculations; inhibitor isomers

1. INTRODUCTION

Conjugated imines, also known as Schiff bases, are obtained by the condensation reaction between aromatic aldehydes and amines. These compounds display important properties in corrosion inhibition [1-5]. Functionalized Schiff bases have been studied to evaluate their inhibition efficiency. In order to obtain a good inhibitory effect, Schiff bases should contain electronegative atoms such as nitrogen, oxygen and sulfur [1-6], which could provide electrons, and aromatic rings such as phenyl, pyridine, etc. [7-10] for transferring the electrons from these atoms. The effectiveness of a corrosion inhibitor is related with its ability to donate electrons. This desirable ability can be related to the energy of the frontier molecular orbitals (HOMO and LUMO) and the electric charges of the groups

forming the molecular structure. Recently, the inhibitory properties of several Schiff base compounds have been studied from both theoretical and experimental perspectives [11-17]. These studies employed quantum chemical calculations based on DFT methods [12-17]. The relationship between the molecular structure and the inhibitory efficiency was analyzed for various Schiff bases containing phenol and diphenol [12], and also for several derivatives containing aldehydes such as benzaldehyde, salicylaldehyde, vanillin and cinnamaldehyde [13, 14]. The results showed that the inhibition efficiency was increased with higher HOMO energy and lower LUMO energy and with higher gap energy [12-14].

In other studies, Chen et al. [15-17] evaluated the inhibition efficiency with the HOMO and LUMO energies and the net charges of the groups and atoms in the Schiff bases by means of regression equations. The most effective parameter in inhibition efficiency was the total charge of the $-\text{CH}=\text{N}-$ group, with the inhibition efficiency having a good linear relationship with the HOMO energy, the charge of the N atom of the $-\text{CH}=\text{N}-$ group, and the absolute electronegativity of the Schiff bases derivatives of benzylidene [15], mercapto-triazole [16], and salicylidene-ethylenediamine [17].

In this work, we investigated the properties of a series of isomers of the Schiff base (*E*)-2-(2-hydroxybenzylideneamino)phenylarsonic acid (SBAs-OH) and their abilities to inhibit corrosion. These compounds contain in their structures hydroxy-substituted and arsonic-substituted phenyl rings linked by the characteristic imine group ($-\text{CH}=\text{N}-$). We were particularly interested in the role of the position of the hydroxy substituent ($-\text{OH}$) on the phenyl ring in affording effective inhibitors of corrosion. Structural parameters, frontier energy levels, dipole moments, and charge distributions were obtained by DFT methods for each isomer. Using this information as parameters of inhibition efficiency, we calculated a regression equation that described the corrosion inhibition efficiency (IE), following the methodology implemented in [15-17]. The relationship between the calculated IE and the molecular structure of the different isomers was analyzed. We also compared the theoretical IE of the SBAs-OH series with previous results for other substituted Schiff bases.

2. CALCULATION METHOD

Theoretical DFT calculations were carried out on the Schiff base SBAs-OH. Density functional theory (DFT), especially since the work of Kohn and Sham [18], is based entirely on the exchange and correlation density functional. Because this functional is not exactly known, it is necessary to use several approximations. The meta-GGAs, examples of this type of functional, are a family of functionals developed by Truhlar and Zhao [19], and they are widely used for studying organic systems. All optimization calculations were performed employing the meta-GGAs functional M06L [20]. Five different isomers were calculated for different positions of the hydroxyl group on the phenyl ring and their molecular structures and numerical conventions are shown in Figure 1. The basis set used for the arsenic atom was the effective core potential basis set of Hay and Wadt, LanL2DZ [21] and the Dunning basis set cc-pVTZ [22] was used for the N, C, H and O atoms. Also the vibrational

frequencies were calculated at the same theory level as the optimization calculations to ensure the minimum energy structures.

Energy levels of the HOMO and LUMO orbitals were calculated at DFT/ M06L/cc-PVTZ theory level and using LanL2DZ for the As atom. The energy gap was calculated as $\Delta E = \epsilon_{\text{LUMO}} - \epsilon_{\text{HOMO}}$, and reported in eV. The net charges of the atoms and groups were calculated as Mulliken charge populations. The Fukui functions were calculated from the density functional theory of the electronic structure of the molecules [23].

The condensed Fukui function is the best parameter to study for measurement of the local selectivity of a corrosion inhibitor. The global electrophilicity index was introduced by Parr *et al.* [24] as the ratio between the chemical potential squared and twice the absolute hardness, and is expressed by ω . This index measures the propensity of chemical species to accept electrons. A good nucleophile is characterized by a lower value of ω , while a good electrophile is characterized by a high value of ω . This new reactivity index measures the stabilization in energy that occurs when the system acquires an additional electronic charge ΔN from the environment.

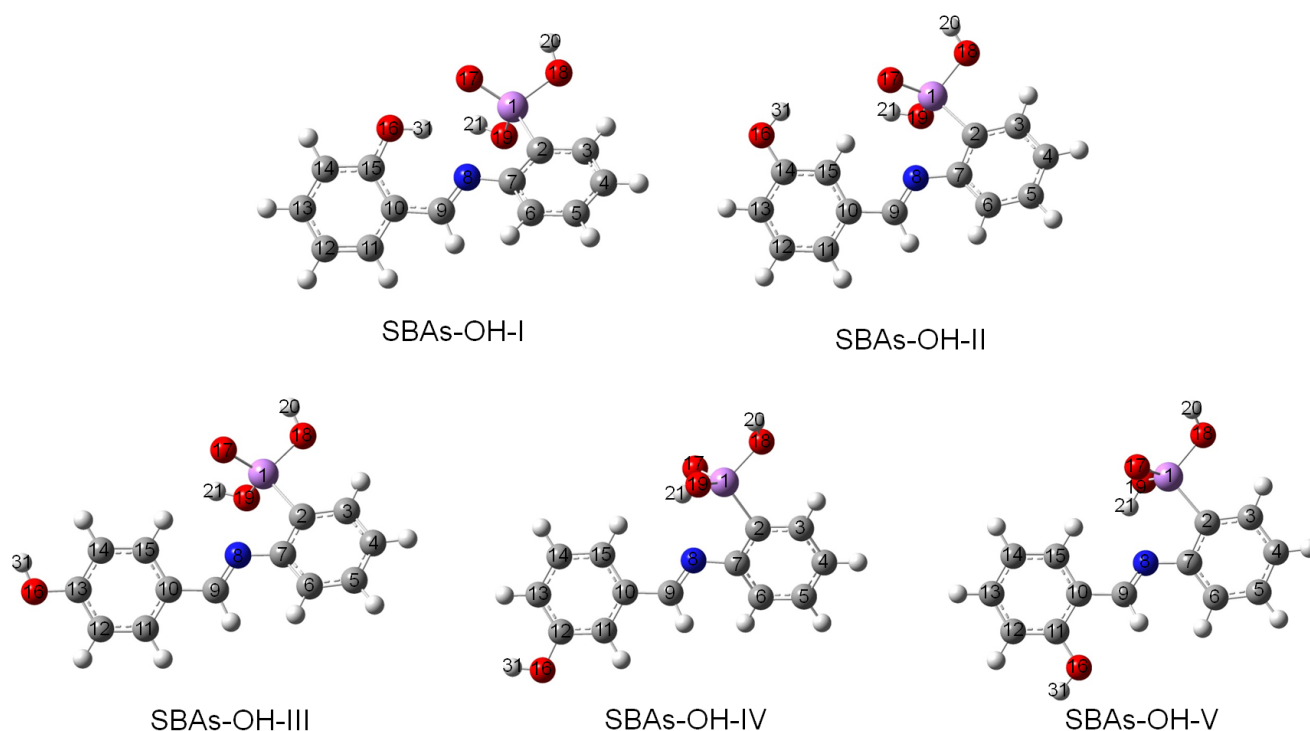


Figure 1. Optimized molecular structures and numerical conventions of the isomers of SBAs-OH calculated at M06L level theory and using LanL2DZ for As and cc-pVTZ basis set for all other atoms. Red= oxygen, blue= nitrogen, gray= carbon, pink= arsenic, white= hydrogen.

An accepted criterion to describe the reactivity is the Hard and Soft Acids and Bases (HSAB) principle. Under the concepts of DFT, it is possible to reveal the underlying mechanism that describes how a molecular system responds to electronic perturbation, considering the structure-property relationship. DFT provides a rigorous theoretical framework for the analysis and interpretation of the electronic structure of different molecules. The Fukui function is an electron density-based concept

that describes the corresponding sensitivity of a molecular system to electronic perturbations [23]. The Fukui function is defined as the change of the electronic density with respect to the number of electrons (N), with a constant external potential: $f^-(r) \equiv \left(\frac{\partial \rho(r)}{\partial N} \right)_{V(r)}$

Due to the discontinuity of the derivative expression with respect to N , the following Fukui function $f^-(r)$ can be calculated using the finite difference approximation as follows:

$$f^-(r) = \rho_N(r) - \rho_{N-1}(r),$$

where $\rho_N(r)$ and $\rho_{N-1}(r)$ are the electronic densities of the system with N and $N+1$ electrons, respectively, based on ground state geometry of the N electron system. The HSAB principle can then be applied considering the magnitude of the Fukui function in each site in the molecule, postulating in our case that the maximum values of $f^-(r)$ indicate regions in the molecule suitable for attack by an electrophile. All the calculations were carried out in the Gaussian 09 program [25].

3. RESULTS AND DISCUSSION

3.1. Molecular structure of SBAs-OH isomers

The corrosion inhibition efficiency can be closely related to the molecular structure of the inhibitor. The inhibitors studied herein include several containing oxygen atoms in their structures (as methoxy, nitro, hydroxy) and these groups may serve as electron suppliers. Within the structure of these inhibitors are two groups containing oxygen atoms, the hydroxy group and the arsonic acid, each attached to a phenyl ring. Calculations of the full optimization at M06L were carried out using the cc-pVTZ basis set for all atoms, except for the As atom, which was calculated using the LanL2DZ basis set and an effective core potential. The calculations of the vibrational frequencies showed that all structures corresponded to the minimum energy geometries, with the isomer SBAs-OH-I with the $-OH$ group attached in the *ortho*-position being the most stable (Figure 1). In Table 1, representative parameters are compared for the five isomers. The X-ray data of isomer SBAs-OH-I are included for comparison [26].

The calculated parameters agreed well with those reported by X-ray data (Table 1). In most of the cases, the calculated bond distances were only slightly different than the X-ray data. The bond angles exhibited slight differences. The dihedral angles are determinants for the geometric and energetic stability of the molecule. The dihedral angles indicating the planarity of the structure were C10–C9–N8–C7 (torsion between the substituted phenyl ring through the central central imine group ($-CH=N-$)), C9–N8–C7–C2 (coplanarity of the $AsO(OH)_2$ -substituted phenyl ring with the central imine group ($-CH=N-$)), and C15–C10–C9–N8 (coplanarity of the OH -substituted phenyl ring with the central imine group ($-CH=N-$)) (Figure 1). The value of the C10–C9–N8–C7 angle indicated an arrangement of the phenyl rings close to 180° through the central imine group ($-CH=N-$) in all isomers. However, the structure showed great conformational flexibility depending of the torsions of the substituted phenyl rings about single bonds C10–C9 and N8–C7 [26]. The OH -substituted phenyl ring was found to be more coplanar in isomer SBAs-OH-I, while the $AsO(OH)_2$ -substituted phenyl

ring was found to be more coplanar in isomer SBAs-OH-II, with respect to the central imine group (–CH=N–). Isomer SBAs-OH-V was found to be slightly twisted in both substituted-phenyl rings, while SBAs-OH-III and SBAs-OH-IV presented as planar structures. The change of position of the –OH group generated structures with relative energies between 6.0 and 8.4 kcal mol⁻¹ (Table 2).

3.2. Frontier molecular orbitals, charges and dipole moments of SBAs-OH isomers

Chemical phenomena in reactions are accompanied by interactions between the electrons located in the frontier molecular orbitals, *i.e.*, HOMO and LUMO. In the corrosion process, the HOMO and LUMO orbitals have been taken into consideration as measurements of electron donating ability and electron affinity, respectively. We therefore calculated the HOMO, LUMO, and the gap energies of the SBAs-OH isomers at DFT/ M06L/cc-PVTZ theory level and using LanL2DZ for the As atom. The larger energy of the HOMO indicated greater electron donor behavior. The isomers with a larger ϵ_{HOMO} were SBAS-OH-I and SBAS-OH-III with -5.69 eV. On the other hand, smaller energy of the LUMO indicated larger electron affinity, as represented by SBAs-OH-II and SBAs-OH-V. While some isomers had a greater tendency to donate electrons, others could accept electrons easier. So, an important indicator for the behavior of a corrosion inhibitor is the gap energy, $\Delta E = \epsilon_{\text{LUMO}} - \epsilon_{\text{HOMO}}$. A smaller ΔE would favor better conditions for the interaction between electron donor inhibitor and the metal surface. The gap energies for the five isomers were close in value, ranging from 2.83–3.01 eV, and being slightly larger for the isomer SBAs-OH V. Similar values of gap energies have been reported [15–17] for Schiff bases containing methoxy-phenyl, mercapto-triazole, and salicylidene, which were predicted to be good corrosion inhibitors.

Table 1. Theoretical structural parameters of the equilibrium structures of SBAs-OH isomers calculated at the M06L/cc-pVTZ theory level and using LanL2DZ for the arsenic atom. The numbering convention is shown in Fig. 1. Internuclear distances in (Å), and valence and dihedral angles in (°)

Parameter	X-ray data ^a	SBAs-OH-I	SBAs-OH-II	SBAs-OH-III	SBAs-OH-IV	SBAs-OH-V
C9=N8	1.2862	1.2864	1.2780	1.2803	1.2768	1.2800
C10–C9	1.4449	1.4328	1.4505	1.4428	1.4516	1.4468
N8–C7	1.4142	1.3929	1.3888	1.3913	1.3936	1.3931
C2–As	1.9052	1.9022	1.9170	1.9147	1.9152	1.9143
O16–C15	1.3534	1.3321	1.3537 ^b	1.3519 ^c	1.3581 ^d	1.3582 ^e
O17–As	1.6524	1.6178	1.6206	1.6176	1.6166	1.6174
O18–As	1.7163	1.7621	1.7623	1.7643	1.7638	1.7640
O19–As	1.7144	1.7712	1.7690	1.7691	1.7676	1.7678
O16–H31	0.8338	0.9785	0.9631	0.9614	0.9606	0.9607
O18–H20	0.7776	0.9606	0.9606	0.9607	0.9607	0.9607
O19–H21	0.8027	0.9631	0.9631	0.9640	0.9641	0.9642
N8...H21	3.7488	3.1573	2.5110	2.4174	2.4340	2.4194
C9–N8–C7	120.75	121.40	126.10	124.36	123.98	123.54

C10–C9–N8	122.60	123.68	119.85	121.26	121.19	120.62
C15–C10–C9	122.10	123.20	119.07	120.82	120.67	120.83
O16–C15–C10	121.47	124.29	122.18 ^b	122.35 ^c	122.78 ^d	122.12 ^e
C15–O16–H31	104.39	112.17	108.56 ^b	109.06 ^c	108.93 ^d	108.90 ^e
O17–As–C2	118.91	120.76	123.51	122.32	121.74	121.80
O18–As–C2	103.03	98.98	98.87	99.71	99.56	99.80
O19–As–C2	107.02	105.83	105.12	104.70	104.77	104.76
H20–O18–As	107.52	109.96	109.17	108.65	108.80	108.70
H21–O19–As	111.01	107.50	107.66	106.80	107.05	106.77
C4–C3–C2–As	177.91	177.57	178.61	178.96	179.01	178.97
C9–N8–C7–C2	-179.69	-155.84	-173.10	-166.62	-164.36	-162.50
C10–C9–N8–C7	-179.99	-178.92	-174.63	-175.74	-177.25	-175.56
C15–C10–C9–N8	1.09	0.41	13.53	12.61	14.34	16.54
O16–C15–C10–C11	-177.87	-179.68	-178.80 ^b	-179.82 ^c	-179.53 ^d	-179.60 ^e
H31–O16–C15–C10	-2.15	-5.48	-1.28 ^b	-0.24 ^c	-0.15 ^d	-2.36 ^e
O17–As–C2–C3	-115.61	-120.91	-114.70	-112.85	-112.19	-112.68
O18–As–C2–C3	8.76	6.42	10.65	12.57	13.31	12.80
O19–As–C2–C3	119.02	110.62	111.67	113.69	114.44	114.06
H20–O18–As–C2	-108.68	-164.48	-155.55	-150.00	-150.63	-150.10
H21–O19–As–C2	161.74	118.32	76.13	68.63	70.41	68.91

^a X-ray data for the SBAs-OH-I ^b With C14, C15 and C10 ^c With C13, C14 and C15 ^d With C12, C13 and C14 ^e With C11, C12 and C13

Table 2. Relative energies, HOMO, LUMO and gap energies, and coefficients of the atoms contributing to the HOMO and LUMO orbitals of SBAs-OH isomers calculated at M06L/cc-pVTZ theory level and using LanL2DZ for arsenic atom. The labelling convention for groups is shown in Fig. 1.

	SBAs-OH-I	SBAs-OH-II	SBAs-OH-III	SBAs-OH-IV	SBAs-OH-V
$E_{\text{rel}}(\text{kcal mol}^{-1})$	0.00	6.07	6.26	8.40	7.52
$\epsilon_{\text{HOMO}}(\text{eV})$	-5.685	-5.794	-5.690	-5.837	-5.811
$\epsilon_{\text{LUMO}}(\text{eV})$	-2.797	-2.961	-2.735	-2.894	-2.797
$\Delta E(\text{eV})$	2.89	2.83	2.96	2.94	3.01
Coefficients of the atoms contributing to the HOMO and LUMO orbitals					
HOMO					
N8 (6py)	-0.0797	-0.0802	-0.1631	-0.1058	0.1324
(7py)	-0.0823	-0.0722	-0.1392	-0.0903	0.1113
C10 (6py)	0.1301	0.0932	0.1784	0.1105	-0.1700
(7py)	0.0794	0.0529	0.1308	0.0767	-0.1425
C11 (5py)	-0.0315	0.1634	0.0587	-0.0661	-0.1346
(6py)	-0.0401	0.2107	0.0768	-0.0883	-0.1851
C12 (6py)	-0.1401	0.0512	-0.1238	-0.1724	-0.0958
(7py)	-0.1124	0.0299	-0.1034	-0.0834	-0.0744
C13 (5py)	-0.0431	-0.1298	-0.1190	-0.1322	0.0823

	(6py)	-0.0566	-0.1715	-0.1633	-0.1747	0.1064
C14	(5py)	0.0770	-0.1282	-0.0735	0.0453	0.1361
	(6py)	0.1037	-0.1763	-0.0985	0.0588	0.1762
C15	(6py)	0.1270	-0.1264	0.0933	0.2106	0.0325
	(7py)	0.0674	-0.1058	0.0705	0.1582	0.0273
O16	(6py)	-0.1352	0.2148	0.1631	0.1901	0.1873
	(7py)	-0.1182	0.1998	0.1570	0.1804	0.1785
LUMO						
C4	(6py)	-0.0696	-0.1404	-0.1374	-0.1357	-0.1319
	(7py)	-0.1032	-0.1648	-0.1641	-0.1594	-0.1538
C6	(7py)	-0.0103	0.1648	0.1551	0.1485	0.1410
	(7pz)	-0.1248	0.0555	0.1219	0.1219	0.1902
C7	(4s)	0.1094	0.1550	0.1905	0.1771	0.2211
	(7py)	-0.1590	-0.1499	-0.1559	-0.1494	-0.1455
N8	(6py)	-0.1409	-0.1811	-0.1755	-0.1831	-0.1787
	(7py)	-0.1675	-0.2122	-0.2066	-0.2101	-0.2075
C9	(6py)	0.1929	0.2549	0.2531	0.2462	0.2400
	(7py)	0.2089	0.2704	0.2651	0.2520	0.2577
C11	(6py)	-0.1036	-0.1203	-0.1257	-0.1372	-0.1330
	(7py)	-0.0947	-0.1280	-0.1269	-0.1409	-0.0938
C13	(6py)	0.1172	0.1430	0.1644	0.1428	0.1483
	(7py)	0.1325	0.1672	0.1459	0.1817	0.1728
C15	(6py)	-0.1035	-0.1232	-0.1354	-0.1154	-0.1273
	(7py)	-0.0680	-0.1317	-0.1548	-0.1284	-0.1367

Figure 2 shows the distribution of the frontier molecular orbitals for the five isomers of SBAs-OH Schiff bases. HOMOs and LUMOs showed the same activity centers in all isomers. The HOMO was mainly delocalized on the bonds of the OH-substituted phenyl ring, the N=C bond, and the AsO(OH)₂-substituted phenyl ring. The greatest contributions to the HOMO were from the atoms C10, C11, C12, C13, C14 and C15 in the aromatic ring containing the OH group, N8 of the imine, and O16 of the hydroxy group, according to their coefficients (Table 2). Clearly, the greatest contribution to the HOMO was from the oxygen atom of –OH group in all the isomers. On the other hand, LUMO was main delocalized on the atoms of the OH-substituted phenyl ring, the single central bonds C–C and N–C, and on the bonds of the AsO(OH)₂-substituted phenyl ring, except for the isomer SBAs-OH-II which did not contribute to this orbital. The great contributions to LUMO were those of the C2, C4, C6, and C7 of the AsO(OH)₂-substituted phenyl ring, C11, C13, and C15 of the OH-substituted phenyl ring; N8 and C9 of the imine group also contributed to LUMO (Table 2).

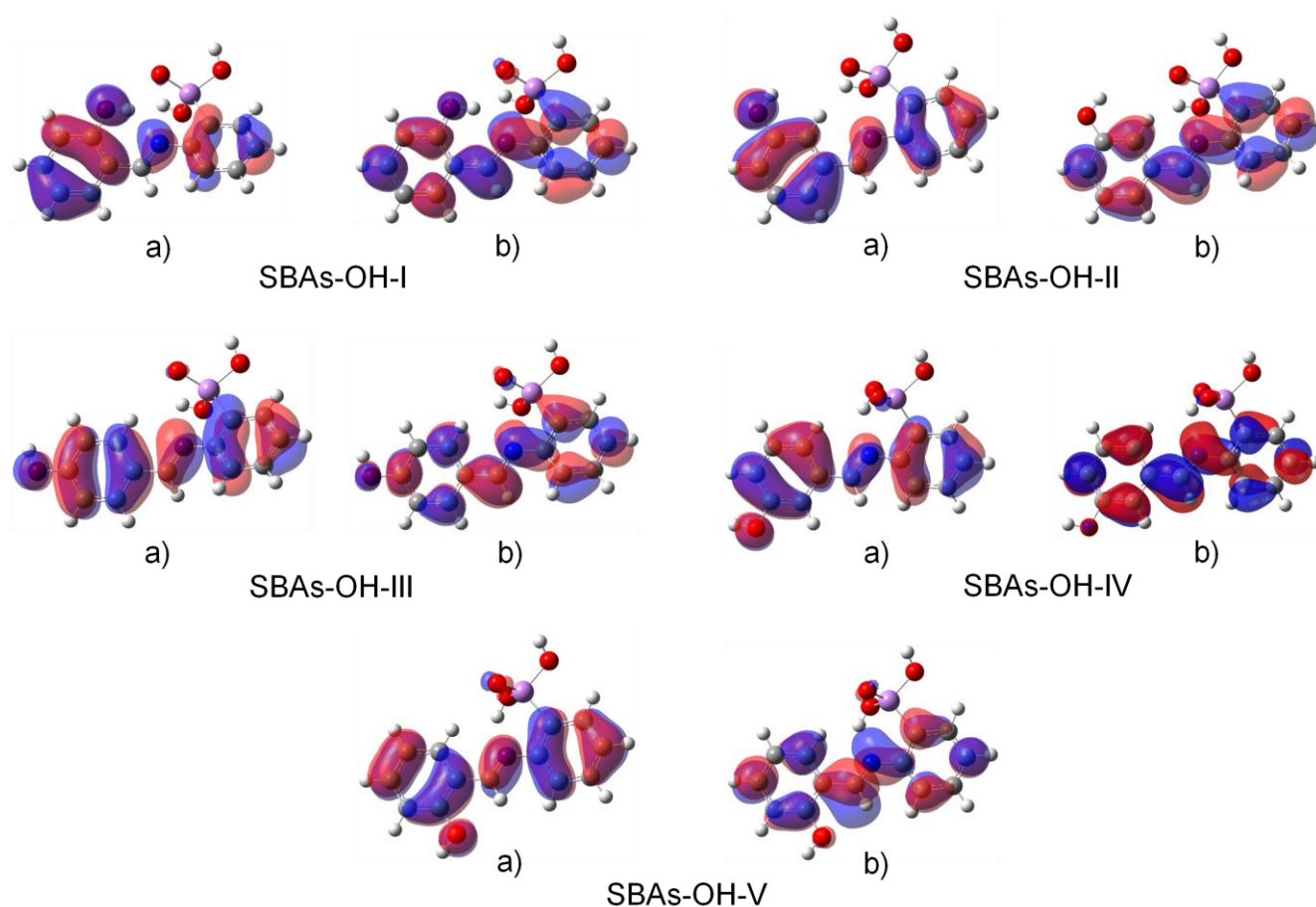


Figure 2. Frontier molecular orbitals: a) HOMO and b) LUMO of the isomers of SBAs-OH calculated at M06L/cc-pVTZ theory level and using LanL2DZ for the arsenic atom.

Table 3. Ionization potential (I), electron affinity (A), electronegativity (χ), hardness (η), softness (σ) and electron transference (ΔN) of five potential SBAs-OH inhibitors.

	SBAs-OH-I	SBAs-OH-II	SBAs-OH-III	SBAs-OH-IV	SBAs-OH-V
I	5.685	5.794	5.690	5.837	5.811
A	2.797	2.961	2.735	2.894	2.797
χ	4.241	4.378	4.213	4.366	4.395
η	1.444	1.416	1.477	1.472	1.417
σ	0.693	0.706	0.677	0.680	0.706
ΔN_{Al}	0.471	0.432	0.470	0.420	0.426
ΔN_{Fe}	0.955	0.926	0.943	0.895	0.920

$\chi_{Al} = 5.6$ eV; $\eta_{Al} = 0.0$ eV; $\chi_{Fe} = 7.0$ eV; $\eta_{Fe} = 0.0$ eV. Reference [27].

Furthermore, the values of the ionization potential, I , and electron affinity, A , are directly related to the energies ϵ_{HOMO} and ϵ_{LUMO} , respectively, as $I = -\epsilon_{HOMO}$ and $A = -\epsilon_{LUMO}$, according to

Koopman's theorem [27]. So, the absolute electronegativity values (χ) and global hardness (η) for each inhibitor can be calculated as: $\chi=(I+A)/2$ and $\eta=(I-A)/2$, while the softness, σ , is the reverse of global hardness: $\sigma=1/\eta$. The χ and η values are used to calculate the fractions of the electrons transferred from the corrosion inhibitor molecule to the metal, named ΔN , as $\Delta N=(\chi_{\text{met}}-\chi_{\text{inh}})/2(\eta_{\text{met}}+\eta_{\text{inh}})$, where the subscripts met and inh refer to metal and inhibitor, respectively. In a first approach, we calculated the ΔN for the five SBAs-OH inhibitors for the transfer of electrons to either Al or Fe atoms (Table 3). Our calculations showed that the five potential inhibitors had a greater tendency to transfer electrons to the Fe atom rather than to Al, with values in the range of 0.895 – 0.955. The five inhibitors were approximately twice as likely to transfer electrons to the Fe atom than to the Al atom.

On the other hand, the net charges of the most negative and most positive atoms are indicators of the distribution of the electrons in the molecule. Mulliken population analysis has been widely used for the calculation of the charge distribution in a molecule [15]. In corrosion inhibitor studies, it has also been important to analyze the net group charges for evaluating the charge distribution of a given functional group. Figure 3 shows the convention for the charge calculation for different groups in the inhibitor molecule. Table 4 shows the values of Mulliken charges of atoms and groups, as well as, the dipole moments of SBAs-OH isomers.

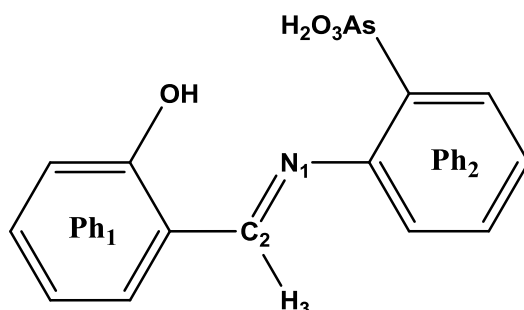


Figure 3. Scheme of the SBAs-OH inhibitor for the charge calculation.

Table 4. Mulliken charges of atoms and groups and dipole moments of SBAs-OH isomers calculated at M06L/cc-pVTZ theory level and using LanL2DZ for arsenic atom. The labelling convention for groups is shown in Fig. 3.

Parameter	SBAs-OH-I	SBAs-OH-II	SBAs-OH-III	SBAs-OH-IV	SBAs-OH-V
Q_{N1}	-0.383	-0.370	-0.384	-0.374	-0.381
Q_{C2}	-0.110	-0.098	-0.092	-0.069	-0.080
Q_{H3}	0.188	0.191	0.187	0.184	0.193
Q_{N1C2H3}	-0.305	-0.277	-0.289	-0.258	-0.268
Q_{OH}	-0.042	-0.110	-0.105	-0.120	-0.116

Q_{Ph1}	-0.535	-0.605	-0.574	-0.626	-0.597
Q_{Ph2}	-0.673	-0.655	-0.681	-0.662	-0.671
$Q_{AsO_3H_2}$	-0.060	-0.043	-0.040	-0.033	-0.036
μ_{tot} (Debye)	3.998	4.277	3.712	4.337	5.8528

3.3. Correlation between frontier molecular orbitals and net charges of SBAs-OH isomers and their corrosion inhibition performance.

To predict the inhibition efficiency (%IE) of our compounds, we used a linear relationship between the various molecular electronic properties calculated for the potential inhibitors and the mean experimental inhibition efficiencies determined experimentally, as determined from electrochemical measurements with previously described organic inhibitors with similar structure. For the individual SBAs-OH isomers containing the structures of *ortho*, *meta*, and *para*-OH-substituted phenyl ring, we used the inhibition efficiency of the corresponding *ortho*, *meta*, and *para* chlorophenylsalicyaldimine compounds [28]. Using the parameters such as HOMO, LUMO, gap energies, Mulliken charges, and dipole moments reported in Tables 2 and 4, we obtained the regression equations for the inhibition efficiency (Table 5).

Table 5. Regression equations of HOMO, LUMO, gap energies, Mulliken charges and dipole moment of SBAs-OH isomers and their corrosion inhibition efficiency.

Variable	Regression equation	R^2
ϵ_{HOMO}	IE= 285.91 + 33.662 ϵ_{HOMO} (1)	0.983
ϵ_{LUMO}	IE=138.96 + 16.139 ϵ_{LUMO} (2)	0.821
ΔE	IE= 20.856 + 25.037 ΔE (3)	0.543
Q_{N1}	IE= - 9.074 - 269.9 Q_{N1} (4)	0.961
Q_{N1C2H3}	IE= 53.696 - 136.14 Q_{N1C2H3} (5)	0.820
Q_{Ph1}	IE= 124.3 + 54.344 Q_{Ph1} (6)	0.836
Q_{Ph2}	IE= -0.996 - 140.79 Q_{Ph2} (7)	0.814
μ_{tot}	IE= 115.76 - 5.630 μ (8)	0.586

The best linear regression coefficients corresponded to the equations (1) and (4), which indicated that the inhibition efficiencies of these Schiff bases increased when the ϵ_{HOMO} and Q_{N1}

increased. By using equations (1) and (8), we calculated inhibition efficiencies for each of the SBAs-OH isomers, as plotted in Figure 4. Values of 94.53, 90.88, 94.37, 89.42 and 90.30% of corrosion inhibition efficiency for SBAs-OH-I, SBAs-OH-II, SBAs-OH-III, SBAs-OH-IV and SBAs-OH-V, respectively, were calculated using equation (1) and the IE% values obtained by using equation (4) were 94.38, 90.91, 94.51, 93.68 and 93.75%, respectively. Although the correlation between ΔE and the percent inhibition efficiency was the worst ($r^2=0.543$), the calculated %IE from equation (3) for isomer SBAs-OH-V was the highest using its high value of gap energy ($\Delta E=3.01$ eV). However, a contradictory result was found using the correlation between μ_{tot} and %IE (equation (8)), obtaining a predicted value of %IE of 82.8% for this isomer. The best correlations were found for equations (1), (2), (4) and (6) for ϵ_{HOMO} , ϵ_{LUMO} , Q_{N1} and Q_{Ph1} which yielded the average values for %IE of 91.9, 93.2 and 93.1 and 92.7%, respectively. These predicted values were within the ranges obtained for similar molecular structures of organic inhibitors using theoretical approaches [12, 15-17].

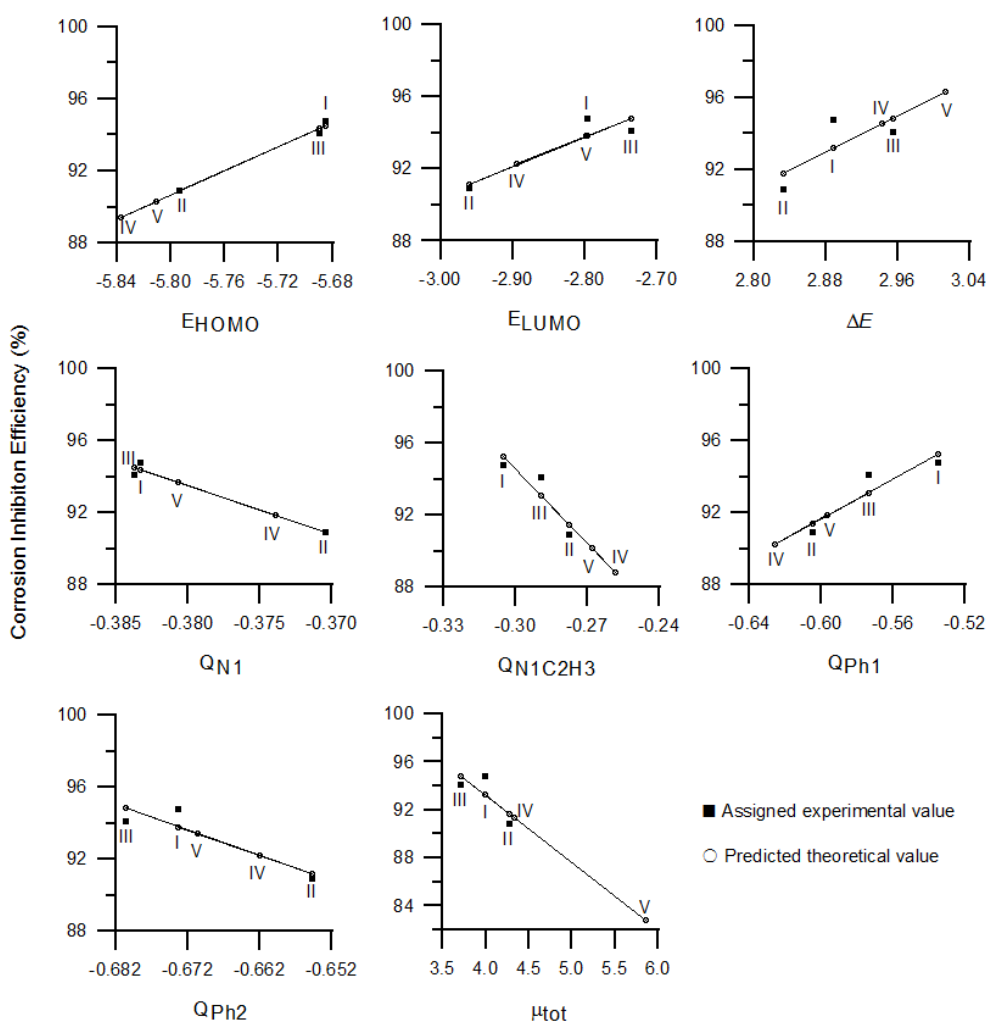


Figure 4. Correlation of theoretical electronic parameters with percent inhibition efficiency of SBAs-OH isomers. The square symbols (■) indicate the correlated values of the theoretical parameters with the values of %IE experimentally assigned by the values previously reported for inhibitors with similar structures [28]. Circle symbols (○) indicate the theoretically predicted values from regression equations in Table 5.

3.4. Fukui functions of SBAs-OH isomers

The condensed negative Fukui function surfaces are illustrated in Figure 5. The zones indicated in black represent the regions where the inhibitor molecule has a major concentration of electrons to donate to the empty d orbitals in the Al or Fe metal. The Fukui function represents the change of the electronic density $\rho(r)$ in a given point with respect to the change in the number of electrons N [29]. For the electrophilic attack to occur, the contributing atoms are likely to be the carbon atoms on the OH-substituted phenyl ring in all isomers, the oxygen atom in the isomer SBAs-OH-I, the nitrogen atom of the imine group of isomer SBAs-OH-III, and a region located in AsO(OH)₂-substituted phenyl ring.

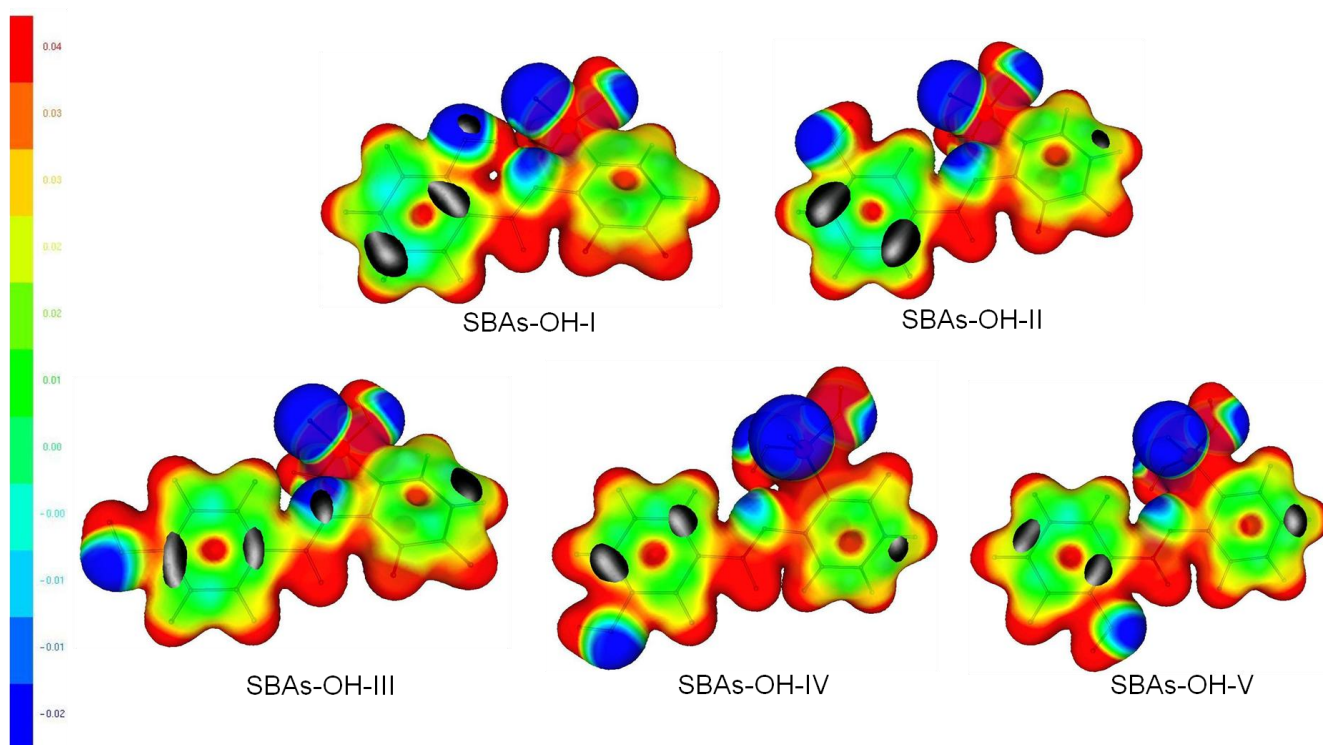


Figure 5. Isosurface plots for the electrophilic form of the Fukui Function $f^-(r)$. The black zones are, associated with the softer regions of the SBAs-OH inhibitors which are likely to give up electronic charge and which are especially reactive toward electron-poor metals.

4. CONCLUSIONS

In this work, a theoretical study of the molecular structure, electron distribution, and the inhibition performance of a series of isomers of novel inhibitor compounds containing a Schiff base was carried out.

Our studies indicated that it is possible to predict the behavior of an agent as an inhibitor of corrosion from the electronic properties such as frontier molecular orbital, atomic charges, dipole

moment, and gap energies. In our particular case, experimental values were not found to corroborate the trend in the series of the isomers calculated. However, interesting relationships between the molecular structure and the inhibition efficiency were found. Minimum energy geometries for SBAs-OH isomers were calculated by using M06L/cc-pVTZ theory level, including the LanL2DZ for As atom. Isomer with the -OH group attached in the *ortho*-position was energetically more stable. Other isomers were obtained with relative energies between 6.0 and 8.4 kcal mol⁻¹. All structures are almost planar presenting slight twists around single bonds, which may be favorable to the electronic delocalization on the inhibitor molecule.

Atoms providing electrons such as the nitrogen of the imine group (-CH=N-) were more effective than arsonic and hydroxy groups linked to aromatic rings in the molecule. The results showed that the corrosion inhibition efficiency was closely related with the ϵ_{HOMO} and ϵ_{LUMO} values, as well as with the atomic charges of the imine group. The OH- and AsO(OH)₂-substituted aromatic rings play a main role in the electronic distribution during the inhibition process. In our case, contrary to expectations, the ΔE parameter was not a determinant in the inhibition prediction. Mulliken charges corroborated the influence of N and O atoms providing electrons from the inhibitor molecule to the metal surface. The SBAs-OH inhibitors showed a greater tendency to transfer electrons to the Fe atom than the Al atom, in a range of $\Delta N = 0.895 - 0.955$. The inhibition efficiency for SBAs-OH inhibitors was theoretically predicted in a range of 82.8-96.3% using the calculated electronic parameters. The best correlations were obtained with the ϵ_{HOMO} and Q_{N1} increases, obtaining the best theoretical inhibition efficiencies of 94.5% for SBAs-OH-I and SBAs-OH-III, respectively. The predicted values in this work are within the ranges obtained for similar Schiff base inhibitors using theoretical approaches. Further experimental and theoretical studies on Schiff bases containing the -AsO(OH)₂ group will be helpful to corroborate the analysis carried out in the present work.

Theoretical information about molecular electronic properties for analyzing the corrosion inhibition performance can be valuable for predicting the structures of new corrosion inhibitor compounds.

ACKNOWLEDGEMENTS

We thank to CONACYT projects 183833 and 157552; PROMEP-SEP (Thematic network of collaboration); and VIEP projects SOMJ-NAT14-I, CHCV NAT-14-G, and PEZM NAT-14-G for supporting the research.

References

1. S. Bilgic, N. Caliskan, *J. Appl. Electrochem.*, 31 (2001) 79.
2. C. Küstü, K. C. Emregül, O. Atakol, *Corros. Sci.*, 49 (2007) 2800.
3. R. A. Prabhu, T. V. Venkatesha, A. V. Shanbhag, G. M. Kulkarni, R. G. Kalkhambkar, *Corros. Sci.*, 50 (2008) 3356.
4. A. M. Abdel-Gaber, M. S. Masoud, E. A. Khalil, E. E. Sheata, *Corros. Sci.*, 51 (2009) 3021.
5. M. Behpour, S. M. Ghoreishi, N. Soltani, M. Salavati-Niasari, *Corros. Sci.*, 51 (2009) 1073.
6. H. D. Lece, K. C. Emregül, O. Atakol, *Corros. Sci.*, 50 (2008) 1460.
7. K. F. Khaled, S. A. Fadel-Allah, B. Hammouti, *Mat. Chem. Phys.*, 117 (2009) 148.

8. T. Arslan, F. Kandemirli, E. E. Ebenso, I. Love, H. Alemu, *Corros. Sci.*, 51 (2009) 35.
9. I. B. Obot, N. O. Obi-Egbedi, *Corros. Sci.*, 52 (2010) 282.
10. J. Zhang, G. Qiao, H. Songqing, Y. Yan, Z. Ren, L. Yu, *Corros. Sci.*, 53 (2011) 147.
11. R. Hasanov, S. Bilge, S. Bilgic, G. Gece, Z. Kilic, *Corros. Sci.*, 52 (2010) 984.
12. H. Ju, Z.-P. Kai, Y. Li, *Corros. Sci.*, 50 (2008) 865.
13. I. Ahamad, R. Prasad, M. A. Quraishi, *Mat. Chem. Phys.*, 124 (2010) 1155.
14. I. Ahamad, C. Gupta, R. Prasad, M. A. Quraishi, *J. Appl. Electrochem.*, 40 (2010) 2171.
15. S. Chen, T. Kar, *Int. J. Electrochem. Sci.*, 7 (2012) 6265.
16. S. Chen, S. Scheiner, T. Kar, U. Adhikari, *Int. J. Electrochem. Sci.*, 7 (2012) 7128.
17. J. Zhu, S. Chen, *Int. J. Electrochem. Sci.*, 7 (2012) 11884.
18. W. Kohn, L. J. Sham, *Phys. Rev.*, 140 (1965) 1133.
19. Y. Zhao, D. G. Truhlar, *Theor. Chem. Account*, 120 (2008) 215.
20. Y. Zhao, D. G. Truhlar, *Chem. Phys. Lett.*, 502 (2011) 1-3, 1-13.
21. W. R. Wadt, P. J. Hay, *J. Chem. Phys.*, 82 (1985) 270.
22. T. H. Dunning Jr., *J. Chem. Phys.*, 90 (1989) 1007.
23. R. G. Parr, W. Yang, *J. Am. Chem. Soc.*, 106 (1984) 4049.
24. R. G. Parr, L. Szentpaly, S. Liu, *J. Am. Chem. Soc.*, 121 (1999) 1922.
25. Gaussian 09, Revision A.1, M. J. Frisch, G. W. Trucks, H. B. Schlegel, G. E. Scuseria, M. A. Robb, J. R. Cheeseman, G. Scalmani, V. Barone, B. Mennucci, G. A. Petersson, H. Nakatsuji, M. Caricato, X. Li, H. P. Hratchian, A. F. Izmaylov, J. Bloino, G. Zheng, J. L. Sonnenberg, M. Hada, M. Ehara, K. Toyota, R. Fukuda, J. Hasegawa, M. Ishida, T. Nakajima, Y. Honda, O. Kitao, H. Nakai, T. Vreven, J. A. Montgomery Jr., J. E. Peralta, F. Ogliaro, M. Bearpark, J. J. Heyd, E. Brothers, K. N. Kudin, V. N. Staroverov, R. Kobayashi, J. Normand, K. Raghavachari, A. Rendell, J. C. Burant, S. S. Iyengar, J. Tomasi, M. Cossi, N. Rega, N. J. Millam, M. Klene, J. E. Knox, J. B. Cross, V. Bakken, C. Adamo, J. Jaramillo, R. Gomperts, R. E. Stratmann, O. Yazyev, A. J. Austin, R. Cammi, C. Pomelli, J. W. Ochterski, R. L. Martin, K. Morokuma, V. G. Zakrzewski, G. A. Voth, P. Salvador, J. J. Dannenberg, S. Dapprich, A. D. Daniels, Ö. Farkas, J. B. Foresman, J. V. Ortiz, J. Cioslowski, D. J. Fox, Gaussian, Inc., Wallingford CT, 2009.
26. M. J. Percino, M. Cerón, M. E. Castro, R. Ramírez, G. Soriano, V. M. Chapela, *J. Mol. Struct.*, Submitted (2014).
27. R. G. Pearson, *Inorg. Chem.*, 27 (1988) 734.
28. K. C. Emregül, R. Kurtaran, O. Atakol, *Corrosion Sci.*, 45 (2003) 2803.
29. P. López, F. Méndez, *Org. Lett.* 6:11 (2004) 1781.